

Synthesis and Evaluation of the Antifungal Sensibility of Novel Thienopyridine 1,2,3-Triazole Derivatives

Ramírez-Villalva Alejandra¹, Cervantes-Rebolledo Claudia², González-González Carlos A.³, Mastachi-Loza Salvador^{3*}

¹Escuela Profesional en Química Farmacéutica Biológica-INIES, Universidad de Ixtlahuaca, CUI. Carretera Ixtlahuaca-Jiquipilco KM 1, Estado de México, 50740, México.

²Escuela Profesional de Médico Cirujano-INIES, Universidad de Ixtlahuaca, CUI. Carretera Ixtlahuaca-Jiquipilco KM 1, Estado de México, 50740, Mexico.

³Departamento de Química Orgánica, Facultad de Química, Universidad Autónoma del Estado de México, Paseo Colón/Paseo Tollocan s/n, Toluca, Estado de México, 50120, México.

*Corresponding author: Mastachi-Loza Salvador, email: mastas20@hotmail.com

Received November 29th, 2022; Accepted August 11th, 2023.

DOI: <http://dx.doi.org/10.29356/jmcs.v68i1.1917>

In honor of Professor Joaquín Tamariz on the occasion of his retirement from the ENCB of the IPN.

Abstract. The family of compounds known as azoles are part of most of the antimicrobial drugs used for the treatment of infections. Within this family triazoles have been extensively studied as pharmacophores with very promising results. In this work, four novel trisubstituted 1,2,3-triazole compounds with a thienopyridine moiety (**1a,b**; **2a,b**) were synthesized through an azide-enolate 1,3-dipolar cycloaddition. Their cheminformatic properties were calculated using simulation software available online such as Molinspiration, Molsoft, Osiris Property Explorer, pkCSM, SwissADME, and GUSA. The results provided important information which allowed us to consider the evaluation of the antifungal activity of these novel compounds. Therefore, the antifungal activity of these compounds was evaluated *in vitro* against four filamentous fungi, including *Aspergillus fumigatus* ATCC 16907, *Trichosporon cutaneum* ATCC 28592, *Rhizopus oryzae* ATCC 10329, and *Mucor hiemalis* ATCC 8690; as well as six species of yeast from the *Candida* genus; *C. albicans* ATCC 10231, *C. utilis* ATCC 9226, *C. tropicalis* ATCC 13803, *C. parapsilosis* ATCC 22019, *C. glabrata* ATCC 34138 and *C. krusei* ATCC 14243. The sensibility studies suggest that compounds **1b**, **2a** and **2b** can be considered candidates for complementary biological studies due to the exhibited antifungal activity.

Keywords: Triazoles; antifungal; cycloaddition; azide-enolate; thienopyridine.

Resumen. La familia de compuestos conocidos como azoles forman parte de la mayoría de los medicamentos utilizados para el tratamiento de infecciones. Dentro de este grupo, los triazoles han sido extensamente estudiados como farmacóforos con resultados muy prometedores. En este trabajo, se sintetizaron cuatro nuevos 1,2,3-triazoles trisustituidos, que incluyen un anillo de tienopiridina en su estructura (**1a,b**; **2a,b**) a través de una cicloadición 1,3-dipolar del tipo azida-enolato. Sus propiedades químicas informáticas fueron calculadas utilizando programas de simulación encontrados en línea como Molinspiration, Molsoft, Osiris Property Explorer, pkCSM, SwissADME y GUSAR. Los resultados obtenidos presentaron información importante que permitió considerar la evaluación de la actividad antifúngica de estos nuevos compuestos. Por lo tanto, esta actividad fue evaluada *in vitro* en cuatro cepas de hongos filamentosos, incluyendo *Aspergillus fumigatus* ATCC 16907, *Trichosporon cutaneum* ATCC

28592, *Rhizopus oryzae* ATCC 10329, and *Mucor hiemalis* ATCC 8690, así como también seis especies de levaduras del género *Candida*; *C. albicans* ATCC 10231, *C. utilis* ATCC 9226, *C. tropicalis* ATCC 13803, *C. parapsilosis* ATCC 22019, *C. glabrata* ATCC 34138 and *C. krusei* ATCC 14243. En estos estudios se observó que los compuestos **1a**, **2a**, y **2b** pueden ser considerados para estudios posteriores de la evaluación biológica debido a la inhibición observada.

Palabras clave: Triazoles; antifúngica; cicloadición; azida-enolato; tienopiridina.

Introduction

The most used class of antifungals are compounds that include an azole moiety [1]. Hence, many triazole and imidazole derivatives have been shown to have a broad spectrum of antibiotic activity which makes them target pharmacophores to counteract mycosis caused by yeast and filamentous fungi [2]. Antifungals such as fluconazole, voriconazole and itraconazole are commonly prescribed drugs for treating invasive fungal infections (IFIs) [3], which continue to be an important cause of morbidity and mortality in immunocompromised patients. These drugs share the presence of a triazole moiety in their structure, which is responsible for the interaction between the molecule and the 14- α -demethylase (the cytochrome P-450 dependent enzyme). Inhibition of this enzyme causes the formation of toxic esters in the fungal membrane; therefore, its permeability is modified and reduces the fungus ability to reproduce [4]. Other nitrogen heterocyclic moieties such as pyridine and thienopyridine have been found in natural compounds and exert significant biological activity in several studies. Some of these compounds have shown important anticancer [5], antibacterial [6], antimalarial, and antifungal biological activity [7]. (Fig. 1).

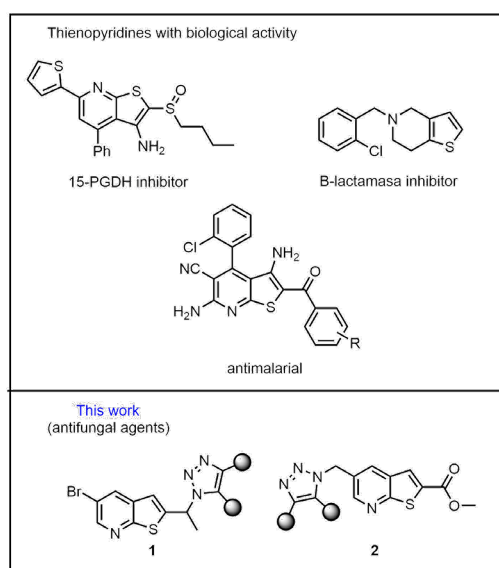


Fig. 1. The novel compounds involve the extremely important 1,2,3-triazole pharmacophoric cores and thienopyridines, a similar feature found in other compounds reported.

The continuous increase of antimicrobial resistance that some fungi are developing makes the design and development of compounds effective for treating these infectious species of clinical importance a constant

necessity (e.g. *Candida albicans*, *C. glabrata* [8], *Aspergillus fumigatus*, *A. niger* [9,10], and *Mucor sp.* and *Cryptococcus neoformans* [10]).

Currently, fungal diseases are of great importance due to the increase of medical conditions that cause immunosuppression in the host and enable the establishment of infections that can range from mild and common superficial infections to potentially fatal invasive infections. Most common pathogens include *Candida* species, which are mainly responsible for invasive candidiasis and candidemia, especially *C. albicans*, *C. glabrata* and *C. krusei* species. The infection usually affects patients admitted to the intensive care unit (ICU) who receive treatments for malignant tumors or stem cell, and organ transplantation [11]. Attention has been focused on these species because of the worldwide increase in resistance they have been displaying against azoles-based drugs and echinocandins [12].

Another important example is *Aspergillus fumigatus* fungus which is the main cause of *Aspergillus* pulmonary disease. An invasive pulmonary aspergillosis (IPA) causes 30-60 % mortality in patients with a compromised immune system [13]. IPA became highly relevant in the COVID-19 pandemic in patients with acute respiratory distress syndrome associated with a high mortality rate that in some reports reached 64.7 % [14].

Mucormycosis is an infection caused by fungi of the Mucorales order which includes several genera. Of this group, *Rhizopus* is associated with around 48 % of cases, followed by *Mucor* which is associated with 14 %. This mycosis affects more patients with HIV, but during the SARS-CoV-2 virus pandemic, cases of coinfection with black fungus, a name given to the lesions caused by mucormycosis, were reported in India with a mortality rate of 30.7 % [15,16].

Similarly, *Trichosporum* species has been reported as the second cause invasive yeast infections in the central nervous system in patients with hematological cancer [17], although it normally causes superficial infections forming nodules along the hair follicle [17]. In the case of *Trichosporum cutaneum* it has been implicated as the causative agent of the summer-type hypersensitivity pneumonitis in Japan [18].

The use of computer software to calculate molecular properties and predict bioactivity is often required in the design of alternative treatments for the above-mentioned infections. Cheminformatic properties have the advantage of predicting the site of action, likely route of administration, pharmacokinetic and pharmacodynamic behavior and potential toxic effects.

Simulation techniques and online servers such as Molinspiration, Molsoft, and the Osiris Property Explorer server, allow the cheminformatic and biological properties of the molecules to be known. These include the partition coefficient, the polar surface area, the number of rotating bonds, hydrogen bond acceptors (HBA), hydrogen bond donors (HBD) and Lipinski rules (Molinspiration and Molsoft). Then the best route of administration can be predicted with the gathered data [19]. Similarly, the pharmacokinetic properties of absorption, distribution, metabolism, excretion, and toxicity (ADMET) can be predicted from the online tool pkCSM and SwissADME. Another important aspect is to know the possible toxicological effects that the compounds may have, for which the Osiris Property Explorer compares molecular properties of the designed compounds with properties of known drug molecules to assess their possible tumorigenic or mutagenic risks [20].

Experimental

Flash column chromatography

SiO₂ 60 (230–400 mesh). TLC: Silica-gel plates (SiO₂; 0.20-mm thickness); visualization with UV light at 254 nm. *m.p.*: Fischer-Johns Scientific melting point apparatus. ¹H- and ¹³C-NMR spectra: Bruker Avance 300 MHz and Varian 500 MHz; δ in ppm rel. to Me₄Si as an internal standard, *J* in Hz. MS: The results were collected using a direct insertion probe and the electron impact ionization method on a Shimadzu GCMS-QP2010 Plus instrument; results are reported in *m/z* (rel. %).

General procedure for the synthesis of the triazole derivatives

The corresponding azide **4** or **6** (0.15 mmol) and the ketone **7 a-c** (0.15 mmol) were dissolved in anhydrous DMF (3 mL) under a nitrogen atmosphere. Then, DBU (0.3 mmol) was added, and the resulting

mixture was stirred at 50–60 °C until reaction completion (monitored through TLC ~24h). Afterwards the solution was cooled to room temperature under continuous stirring. Then, DMF was removed with extractions using a brine solution and EtOAc. The combined organic extracts were filtered and dried over anhydrous Na₂SO₄. Finally, the extracts were concentrated under reduced pressure and the crude reaction mixture was purified by flash chromatography with EtOAc/hexane 7:3.

5-bromo-2-(1-(5-(p-tolyl)-4-tosyl-1H-1,2,3-triazol-1-yl) ethyl)thieno[2,3-b]pyridine (1a).

Following the general procedure, azide **4** (0.042 g, 0.15 mmol) and ketone **7a** (0.043 g, 0.15 mmol) were dissolved in anhydrous DMF (3 mL). DBU (0.044 mL, 0.3 mmol) was added, and the solution was stirred for 24 h at 50–60°C. The mixture was extracted with EtOAc (3x10 mL) and the crude extract was purified by flash column chromatography to afford a white solid **1a** (0.043 g, 52 %), m.p. 152–154 °C. ¹H NMR: (30 MHz, CDCl₃) δ = 8.68 (d, *J* = 2.4 Hz, 1H), 8.29 (d, *J* = 8.0 Hz, 2H), 8.28 (s, 1H), 8.12 (d, *J* = 8.8 Hz, 2H), 7.99 (s, 1H), 7.78 (s, 1H), 7.72 (d, *J* = 8.8, 2H), 7.33 (d, *J* = 8.0 Hz, 2H), 4.75 (d, *J* = 4.5 Hz, 1H), 2.93 (s, 3H), 2.86 (s, 3H), 2.68 – 2.61 (m, 3H) ppm. ¹³C NMR (75 MHz, CDCl₃) δ = 162.6, 161.4, 150.5, 145.5, 135.3, 134.1, 130.5, 130.1, 128.5, 125.7, 124, 117.2, 64.2, 26.7, 21.8 ppm. MS [EI⁺] *m/z* (%) calculated for C₂₅H₂₁BrN₃O₂S₂: 552 [M]⁺ (15), 149 (28), 71 (28), 57 (65), 41 (59).

(1-(1-(5-bromothieno[2,3-b]pyridin-2-yl)ethyl)-5-phenyl-1H-1,2,3-triazol-4-yl)(phenyl)methanone (1b).

Following the general procedure, azide **4** (0.042 g, 0.15 mmol) and ketone **7b** (0.043 g, 0.15 mmol) were dissolved in anhydrous DMF (3 mL). DBU (0.044 mL, 0.3 mmol) was added, and the solution was stirred for 24 h at 50–60°C. The mixture was extracted with EtOAc (3x10 mL) and the crude extract was purified by flash column chromatography to afford a yellow solid **1b** (0.034 g, 47 %), m.p. 138–140 °C. ¹H NMR (300 MHz, CDCl₃) δ = 8.58 (d, *J* = 2.3 Hz, 1H), 8.13 (s, 1H), 7.88 (s, 2H), 7.80 (s, 1H), 7.51 – 7.40 (m, 2H), 7.39 – 7.25 (m, 6H), 5.53 (s, 1H), 2.27 (s, 3H) ppm. ¹³C NMR (75 MHz, CDCl₃) δ = 191.4, 147.8, 145.5, 145.1, 139.7, 134.9, 133.7, 133.1, 130.1, 129.6, 129.3, 128.1, 125.8, 125.3, 123.6, 119.1, 116.8, 63.7, 21.3 ppm. MS [EI⁺] *m/z* (%) calculated for C₂₄H₁₇BrN₄O₂S: 488 [M]⁺ (7), 121 (31), 84 (100), 57 (31), 47 (52), 35 (47).

methyl-((4-benzoyl-5-phenyl-1H-1,2,3-triazol-1-yl)methyl)thieno[2,3-b]pyridine-2-carboxylate (2a).

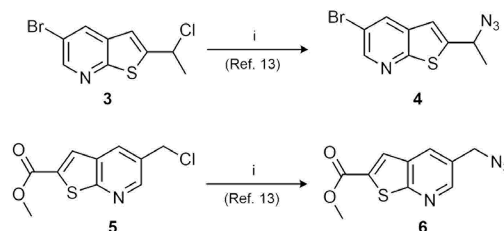
Following the general procedure, azide **6** (0.042 g, 0.15 mmol) and ketone **7b** (0.043 g, 0.15 mmol) were dissolved in anhydrous DMF (3 mL). DBU (0.044 mL, 0.3 mmol) was added, and the solution was stirred for 24 h at 50–60°C. The mixture was extracted with EtOAc (3x10 mL) and the crude extract was purified by flash column chromatography to afford a yellow solid **2a** (0.036 g, 53 %), m.p. 219–221 °C. ¹H NMR (300 MHz, CDCl₃) δ = 8.30 – 8.20 (m, 5H), 7.90 (d, *J* = 3.7 Hz, 2H), 7.74 (s, 1H), 7.59 – 7.51 (m, 1H), 7.52 – 7.37 (m, 4H), 5.59 (s, 2H), 2.87 (s, 3H) ppm. ¹³C NMR (75 MHz, CDCl₃) δ = 177.7, 162.6, 137.0, 133.1, 132.1, 130.7, 130.5, 129.8, 129.8, 129.7, 129.1, 128.3, 128.3, 127.7, 126.8, 126.2, 126.1, 52.9, 49.7 ppm. MS [EI⁺] *m/z* (%) calculated for C₂₅H₁₈N₄O₃S: 454 [M]⁺ (9), 235 (35), 161 (80), 57 (35), 41 (38)

methyl 5-((4-cyano-5-phenyl-1H-1,2,3-triazol-1-yl) methyl)thieno[2,3-b]pyridine-2-carboxylate (2b).

Following the general procedure, azide **6** (0.042 g, 0.15 mmol) and ketone **7c** (0.043 g, 0.15 mmol) were dissolved in anhydrous DMF (3 mL). DBU (0.044 mL, 0.3 mmol) was added, and the solution was stirred for 24 h at 50–60°C. The mixture was extracted with EtOAc (3x10 mL) and the crude extract was purified by flash column chromatography to afford a yellow solid **2b** (0.025 g, 45 %), m.p. 205–207 °C. ¹H NMR (300 MHz, CDCl₃) δ = 8.32 (d, *J* = 2.2 Hz, 1H), 7.89 (d, *J* = 2.2 Hz, 1H), 7.65 – 7.48 (m, 3H), 7.42 – 7.30 (m, 3H), 5.67 (s, 2H), 2.86 (s, 3H) ppm. ¹³C NMR (75 MHz, CDCl₃) δ = 162.6, 147.1, 143.9, 142.2, 133.0, 131.9, 131.7, 129.9, 129, 128.9, 126.8, 126.1, 123.1, 121.3, 50.3, 49.7 ppm. MS [EI⁺] *m/z* [M]⁺ calculated for C₁₉H₁₃N₅O₂S: found 375.0793 [M]⁺ (23.6), 366.9792 (17.8), 354.9792 (20.1).

Results and discussion

In the initial part of this study, the synthesis of azides **4** and **6** was key for introducing the thienopyridine core (Scheme 1). Thus, the synthesis of the derivatives was achieved through nucleophilic substitution of the halogenated thienopyridine analogs **3** and **5** with sodium azide. The reaction proceeded with moderate yields and the compounds were easily purified by chromatography. The introduction of the azide moiety was confirmed by the IR spectra where the characteristic signal for the $-N=N=N$ stretch was identified as a strong sharp signal between $2100-2200\text{ cm}^{-1}$.



Scheme 1. Reagents and conditions: (i) NaN_3 (1.1 eq), DMF anh., $60\text{ }^\circ\text{C}$, 12 h, N_2

Once the desired azides were synthesized, the next step was their transformation into the corresponding triazoles **1a,b** and **2a,b**. One of the most important methodologies for obtaining a 1,2,3-triazole core, is the Copper-catalyzed azide-alkyne cycloaddition (CuAAC) [21]. However, other strategies have emerged with the objective of providing new alternatives with a greener approach. We previously reported a novel synthetic protocol to afford the efficient assembly of 1,4,5-trisubstituted 1,2,3-triazoles through an azide-enolate cycloaddition [22]. Thus, thienopyridine triazoles **1a,b** and **2a,b** were synthesized by the efficient 1,3-dipolar cycloaddition between azide **4** and **6** and different enolates prepared *in situ* from ketones **7** under basic catalysis using 1,8-Diazabicyclo[5.4.0]undec-7-ene (DBU). Table 1 summarizes the results from the cycloaddition. The structure of this novel compounds was confirmed by spectroscopical, and spectrometric methods. All compounds were afforded in moderate yields.

Table 1. Synthesis of thienopyridines and imidazole linked-1,2,3-triazoles from azide **4** and **6** by coupling with active ketones **7**.

| Entry ^a | Ketone | Triazole ^b (Yield%) ^c |
|--------------------|---|---|
| 1 | 6a : $\text{R}_1 = 4\text{-CH}_3\text{Ph}$; $\text{R}_2 = \text{SO}_2\text{-4-Tolyl}$ | 1a : 52 |
| 2 | 6b : $\text{R}_1 = \text{Ph}$; $\text{R}_2 = \text{COPh}$ | 1b : 47 |
| | | |
| Entry ^a | Ketone | Triazole ^b (Yield%) ^c |
| 1 | 6b : $\text{R}_1 = \text{Ph}$; $\text{R}_2 = \text{COPh}$ | 2a : 53 |
| 2 | 6c : $\text{R}_1 = \text{Ph}$; $\text{R}_2 = \text{CN}$ | 2b : 45 |

^aReaction conditions: To a solution of azide compound (1.0 eq) and ketone **7** (1.0 eq) in DMF anh. was added (2.0 eq) of DBU. The reaction mixture was stirred at $50\text{--}60\text{ }^\circ\text{C}$ for 12–24 h.

^bConfirmed by $^1\text{H-NMR}$, $^{13}\text{C-NMR}$ and MS.

^cYields refer to chromatographically pure isolated compounds.

Computational studies

Molecular and chemoinformatic properties were obtained using the Molinspiration, Molsoft and Osiris Property Explorer simulators. The predicted property values of compounds **1a,b** and **2a,b** are summarized in Table 2. Based on the Lipinski rules, all compounds have good therapeutic potential. Only compounds **1a** and **1b** showed violations for the rule of five. However, all compounds displayed HBA and HBD values less than 10 and 5, respectively which indicates good drug permeation [23]. Moreover, triazole derivatives having a molecular weight of less than 500 g/mol and a logP value of less than 5, indicate that the permeability of the compounds through oral administration is favored. In the case of compound **1a** with molecular weight more than 500 and with a logP that exceeds 5, shows a pair of violation to the Lipinski rules but still the compound can be considered for oral administration, or it could be administered by another route, for example parenteral, intravenous or intraperitoneal.

Table 2. Molecular and chemoinformatic properties of compounds **1** and **2**.

| Properties | 1a | 1b | 2a | 2b |
|------------------------------------|--|---|---|---|
| MF | C ₂₅ H ₂₁ BrN ₄ O ₂ S ₂ | C ₂₄ H ₁₇ BrN ₄ OS | C ₂₅ H ₁₈ N ₄ O ₃ S | C ₁₉ H ₁₃ N ₅ O ₂ S |
| MW | 553.51 | 489.39 | 454.50 | 375.40 |
| No. HBA | 6 | 5 | 7 | 7 |
| No. HBD | 0 | 0 | 0 | 0 |
| PSA | 77.75 | 60.68 | 86.99 | 93.71 |
| LogP | 6.37 | 6.15 | 4.62 | 3.26 |
| δ | 1.34 ±0.1 | 1.29 ±0.1 | 1.37 ±0.1 | 1.42 ±0.1 |
| ST | 51.9 ±0.1 | 52.1 ±0.1 | 57.0 ±0.1 | 60.9 ±0.1 |
| Polarizability | 55.32 | 50.12 | 51.08 | 41.55 |
| MR | 139.57 | 126.42 | 128.85 | 104.81 |
| MV | 364.3 | 327.1 | 331.6 | 263.4 |
| nrotb | 5 | 5 | 7 | 5 |
| Drug likeness | -10.89 | -1.88 | -2.33 | -7.09 |
| Lipinski's rules Violations | 2 | 1 | 0 | 0 |

MF= Molecular formula, MW= Molecular weight (g/mol), HBA= Hydrogen bond acceptors, HBD: Hydrogen bond donors, PSA= Polar Surface Area (Å²), LogP= Partition coefficient, δ= density (g/cm³), ST= Surface tension, MR= Molar refractivity (cm³), nrotb= No. of rotatable bonds, MV= Molar volume (cm³).

Molinspiration and Osiris Property Explorer simulators were used to predict the bioactivity of compounds against important drug target sites and predict their potential tumorigenic or mutagenic risks, these results are found in Table 3. The chemoinformatic and bioactivity properties together indicate that these structures are of pharmacological interest, mainly at the kinase inhibitor target site in compounds **2a** and **2b**. The major failure in the drug discovery process is the toxicity and according to the predictions, none of the synthesized triazoles should exhibit mutagenic or tumorigenic impacts, as well as negative reproductive effects. Based on the joint results of the chemoinformatic properties, the most promising compounds to have the desired biological activity are compounds **2a** and **2b** (Table 2), since they do not present violations of the Lipinsky's rules and are the ones that present a lower partition coefficient (4.62 and 3.26 respectively). The latter prediction translates in a better availability and distribution of the compound in the organism, and this is supported by the absorption and metabolism data in Table 4.

Table 3. Prediction of bioactivity and toxicity of compounds **1** and **2**.

| Compound | NCL | IE | GPCR | KI | RE | T | M |
|-----------|-------|-------|-------|-------|----|----|----|
| 1a | -0.99 | -0.17 | -0.21 | -0.30 | No | No | No |
| 1b | -0.81 | -0.07 | -0.17 | -0.04 | No | No | No |
| 2a | -0.61 | 0.04 | -0.07 | 0.06 | No | No | No |
| 2b | -0.69 | 0.00 | -0.12 | 0.13 | No | No | No |

*NCL= Nuclear receptor ligand, IE= Enzyme inhibitor, GPCR= GPCR ligand,
KI= Kinase inhibitor, RE= Reproductive effective, T= Tumorigenic, M= Mutagenic.

Chemoinformatic properties related to ADMET processes were predicted using the online predictors pkCSM and SwissADME (Table 4). In ADMET, the absorption properties indicate that the compounds can be administered orally according to the Lipinsky rules. Other predicted properties such as LogP data, intestinal absorption (% absorbed), P-glycoprotein substrate, and skin permeability (logKp) suggest that these compounds have a high degree of therapeutic bioavailability. In addition, neither compound appears to permeate the blood-brain barrier due to its hydrophilicity, making it difficult to treat pathologies that affect the SNC, although they could have effects on other systems.

Table 4. Data of chemoinformatic properties of ADMET processes.

| ADMET | | 1a | 1b | 2a | 2b |
|---------------------|------------------|-----------|-----------|-----------|-----------|
| Absorption | WS | -4.182 | -3.541 | -3.158 | -3.927 |
| | IA (%) | 94.433 | 98.168 | 100 | 97.494 |
| | SP | -2.735 | -2.735 | -2.735 | -2.735 |
| | SGP | No | No | No | No |
| Distribution | BBBP | No | No | No | No |
| | CNSP | -1.719 | -1.705 | -3.422 | -2.453 |
| Metabolism | CYP3A4 inhibitor | Yes | No | Yes | Yes |
| Excretion | TC | -0.078 | 0.088 | 0.339 | 0.295 |

*WS water solubility (log mol/L), IA intestinal absorption, SP skin permeability (logKp), SGP P-glycoprotein substrate, BBBP blood brain barrier permeability (logBB), CNSP CNS permeability (logPS), TC total clearance (log mL/min/kg), OCT2-s transporters organic cation transporter 2 substrates.

Microbiology

The antifungal *in vitro* sensibility study was carried out for compounds **1a,b** and **2a,b** against four filamentous fungi (*Trichosporon cutaneum* ATCC-28592, *Aspergillus fumigatus* ATCC-16907, *Mucor hiemalis* ATCC-8690, and *Rhizopus oryzae* ATCC-10329), as well as in six yeast specimens of *Candida sp.* (*C. albicans* ATCC-10231, *C. krusei* ATCC-14243, *C. utilis* ATCC-9226, *C. tropicalis* ATCC-13803, *C. parapsilopsis* ATCC-22019, *C. glabrata* ATCC-34138) following the Clinical Laboratory Standards Institute (CLSI) guidelines for standardized microbiological methods. The antifungal study for yeasts was determined by the microdilution method M27-A3 [24], whereas method M38-A [25] was used for filamentous microorganisms. Both studies were performed against itraconazole as a reference standard. The minimum inhibitory concentration (MIC) values of the standard and compounds **1a,b** and **2a,b** are expressed in

micrograms per milliliter and were determined in 96-well plates using MOPS (3- [N-morpholino] propanesulfonic acid buffered RPMI-1640 medium, Sigma- Aldrich).

The antifungal activities of the evaluated compounds are summarized in Table 5.

Compound **2a** showed good inhibitory activity against *C. albicans* (MIC= 0.5 µg/mL) although it was at a considerable higher concentration than the standard (MIC= 0.03 µg/mL). On the other hand, **1b** had important activity against *C. glabrata* (MIC= 0.12 µg/mL). Remarkably, MIC of **1b** was better than the MIC of itraconazole (1 µg/mL). Another important observation was the activity of compound **2b** (MIC= 1 µg/mL) which was comparable to the observed MIC for the standard antifungal drug against *Rhizopus oryzae*. Compound **1a**, however, had no important activity against any of the tested microorganisms.

Table 5. *In vitro* antifungal activities of the synthesized compounds (MIC, µg/mL).

| Compound | <i>C. alb</i> | <i>C. uti</i> | <i>C. kru</i> | <i>C. gla</i> | <i>C. par</i> | <i>M. hie</i> | <i>A. fum</i> | <i>T. cut</i> | <i>R. ory</i> |
|-----------------------------|---------------|---------------|---------------|---------------|---------------|---------------|---------------|---------------|---------------|
| 1a | 16 | 16 | 16 | 16 | 16 | 16 | 8 | 16 | 16 |
| 1b | 8 | 16 | 16 | 0.12 | 8 | 16 | 8 | 16 | 16 |
| 2a | 0.5 | 16 | 2 | 16 | 8 | 16 | 16 | 16 | 2 |
| 2b | 8 | 16 | 8 | 16 | 8 | 16 | 8 | 8 | 1 |
| Standard^a | 0.03 | 0.25 | 0.25 | 1 | 0.06 | 4 | 1 | 8 | 1 |

Abbreviations: *C. alb.*, *Candida albicans*; *C. uti.*, *Candida utilis*; *C. kru.*, *Candida krusei*; *C. gla.*, *Candida glabrata*; *C. par.*, *Candida parapsilosis*; *M. hie.*, *Mucor hiemalis*; *A. fum.*, *Aspergillus fumigatus*; *T. cut.*, *Trichosporon cutaneum*; *R. ory.*, *Rhizopus oryzae*.

According to these results, the presence of the COPh group in position 4, as well as the Ph group in position 5 of the triazole heterocycle resulted in an increase of the biological activity against strains of yeasts of *C. albicans* and *C. glabrata*. The results of compound **2b** showed good activity in the *Rhizopus oryzae* strain since it has the same MIC as the reference drug (MIC= 1 µg/mL). These results indicate that the exchange of the group -COPh at position 4 by a group -CN favors the antifungal activity of **2b** against the filamentous fungus.

These outcomes can also be described by susceptibility parameters of yeast according to the document M27-A3 (Table 6). Generally, *C. glabrata* and *C. albicans* showed some susceptibility to the evaluated compounds, meanwhile *C. krusei*, *C. parapsilosis* and *C. utilis* were resistant to all the evaluated compounds according to the breakpoints described in such document.

Table 6. The determination of the sensibility of yeast (according to document M27-A3): Susceptible (S), dose-dependent sensitive (SDD) and resistant (R).

| Compound | <i>C. alb</i> | <i>C. uti</i> | <i>C. kru</i> | <i>C. gla</i> | <i>C. par</i> |
|-----------------------------|---------------|---------------|---------------|---------------|---------------|
| 1a | R | R | R | R | R |
| 1b | R | R | R | S | R |
| 2a | SDD | R | R | R | R |
| 2b | R | R | R | R | R |
| Standard^a | S | SDD | SDD | R | S |

Abbreviations: *C. alb.*, *Candida albicans*; *C. uti.*, *Candida utilis*; *C. kru.*, *Candida krusei*; *C. gla.*, *Candida glabrata*; *C. par.*, *Candida parapsilosis*.

^aItraconazole. Interpretive criteria: Breakpoints (MIC, µg/mL) = 0.12 [S], 0.25–0.5 [SDD], 1[R].

To better relate the antifungal activity of compounds **1a-b** and **2a-b**, **table 7** shows the MIC ratio in $\mu\text{mol/mL}$ concentrations, noting that compound **1b** has a lower MIC ($2.55 \times 10^{-7} \mu\text{mol/mL}$) than the reference substance (itraconazole = $1.41 \times 10^{-6} \mu\text{mol/mL}$) in the *C. glabrata* strain, this is the best result due to the clinical manifestations of this strain and the low amount of antifungal (**1b**) required to inhibit its growth. Compound **2b** presents the lowest MIC in the strains of *Trichosporon cutaneum* and *Rhizopus oryzae*, where the concentration required to inhibit the growth of the strains is slightly higher than that of itraconazole (standard), being $2.13 \times 10^{-5} \mu\text{mol/mL}$ for *Trichosporon cutaneum* and $2.66 \times 10^{-6} \mu\text{mol/mL}$ for *Rhizopus oryzae*. On the other hand, compound **2a** shows better activity inhibiting yeast growth, highlighting the MIC in *C. albicans* ($1.1 \times 10^{-6} \mu\text{mol/mL}$) and in *C. krusei* ($4.4 \times 10^{-6} \mu\text{mol/mL}$), although according to the established sensitivity criteria. by CLSI, both strains are resistant to compound **2a**. Therefore, we could consider the structures of **1b** and **2b** as a leading compounds for the synthesis of new analogues and to continue with *in vivo* and *in vitro* biological tests.

Table 7. *In vitro* antifungal activities of the synthesized compounds (MIC, $\mu\text{mol/mL}$).

| Compound | <i>C. alb</i> | <i>C. uti</i> | <i>C. kru</i> | <i>C. gla</i> | <i>C. par</i> | <i>M. hie</i> | <i>A. fum</i> | <i>T. cut</i> | <i>R. ory</i> |
|-----------------------|-----------------------|-----------------------|-----------------------|-----------------------|-----------------------|-----------------------|-----------------------|-----------------------|-----------------------|
| 1a | 2.89×10^{-5} | 1.44×10^{-5} | 2.89×10^{-5} | 2.89×10^{-5} |
| 1b | 3.26×10^{-5} | 3.26×10^{-5} | 3.26×10^{-5} | 2.55×10^{-7} | 1.63×10^{-5} | 3.26×10^{-5} | 1.63×10^{-5} | 3.26×10^{-5} | 3.26×10^{-5} |
| 2a | 1.1×10^{-6} | 3.5×10^{-5} | 4.4×10^{-6} | 3.5×10^{-5} | 1.76×10^{-5} | 3.5×10^{-5} | 3.5×10^{-5} | 3.5×10^{-5} | 4.4×10^{-6} |
| 2b | 2.13×10^{-5} | 4.26×10^{-5} | 2.13×10^{-5} | 4.26×10^{-5} | 2.13×10^{-5} | 4.26×10^{-5} | 2.13×10^{-5} | 2.13×10^{-5} | 2.66×10^{-6} |
| Standard ^a | 4.4×10^{-8} | 3.54×10^{-7} | 3.54×10^{-7} | 1.41×10^{-6} | 8.8×10^{-8} | 5.66×10^{-6} | 1.41×10^{-6} | 1.13×10^{-5} | 1.41×10^{-6} |

Conclusions

In summary, the azide-enolate 1,3-dipolar cycloaddition afforded the synthesis of four 1,2,3-triazole derivatives (**1a,b** and **2a,b**) in good yields. *In vitro* studies showed that compound **1b** is the most efficient antimicrobial agent in yeasts followed by compounds **2a**, **2b**, and **1a**, since the first (**1b**) was better than itraconazole against *C. glabrata*. The compound **2b** had better activity against filamentous fungi, showing a MIC $1 \mu\text{g/mL}$ in *R. oryzae*. Compounds **2b** and **2a** had better activity against filamentous fungi, being very close to the MIC values of itraconazole. Consequently, these can be considered candidate drugs for future complementary biological studies.

Acknowledgements

Financial support from Secretaría de Investigación y Estudios Avanzados/UAEMéx (grant 5011/2020CIB and grant 4512/2018C) and CONACyT is gratefully acknowledged. The authors want to thank the referees for valuable comments and suggestions. The authors would also like to thank the referees for their valuable comments and suggestions, and M.N. Zavala-Segovia and L. Triana-Cruz (CCIQS UAEMéx–UNAM) for technical support.

References

1. Benhamou, R. I.; Bibi, M.; Steinbuch, K. B.; Engel, H.; Levin, M.; Roichman, Y.; Berman, J.; Fridman, M. *ACS Chem. Biol.* **2017**, *12*, 1769–1777. DOI: <https://doi.org/10.1021/acscchembio.7b00339>.

- 2.(a) Zhang, Y.-Y.; Zhou, C.-H. *Bioorg. Med. Chem. Lett.* **2011**, *21*, 4349–4352. DOI: <https://doi.org/10.1016/j.bmcl.2011.05.042>. (b) Zhang, H.-Z.; Damu, G. L. V.; Cai, G.-X.; Zhou, C.-H. *Eur. J. Med. Chem.* **2013**, *64*, 329–344. DOI: <https://doi.org/10.1016/j.ejmech.2013.03.049>.
- 3.(a) Guillon, R.; Pagniez, F.; Picot, C.; Hédou, D.; Tonnerre, A.; Chosson, E.; Duflos, M.; Besson, T.; Logé, C.; Le Pape, P. *ACS Med. Chem. Lett.* **2013**, *4*, 288–292. DOI: <https://doi.org/10.1021/ml300429p>. (b) Wang, S.; Zhang, L.; Jin, Y.; Tang, J. H.; Su, H.; Yu, S.; Ren, H. *Asian J. Chem.* **2014**, *26*, 2362–2364. DOI: <https://doi.org/10.14233/ajchem.2014.15956>.
4. Yao, B.; Ji, H.; Cao, Y.; Zhou, Y.; Zhu, J.; Lü, J.; Li, Y.; Chen, J.; Zheng, C.; Jiang, Y.; Liang, R.; Tang, H. *J. Med. Chem.* **2007**, *50*, 5293–5300. DOI: <https://doi.org/10.1021/jm0701167>.
- 5.(a) Lucas, S. C. C.; Moore, J. E.; Donald, C. S.; Hawkins, J. L. *J. Org. Chem.* **2015**, *80*, 12594–12598. DOI: <https://doi.org/10.1021/acs.joc.5b01735>. (b) Elansary, A. K.; Moneer, A. A.; Kadry, H. H.; Gedawy, E. M. *Arch. Pharm. Res.* **2012**, *35*, 1909–1917. DOI: <https://doi.org/10.1007/s12272-012-1107-6>.
6. Leal, B.; Afonso, I. F.; Rodrigues, C. R.; Abreu, P. A.; Garrett, R.; Pinheiro, L. C. S.; Azevedo, A. R.; Borges, J. C.; Vegi, P. F.; Santos, C. C. C.; da Silveira, F. C. A.; Cabral, L. M.; Frugulhetti, I. C. P. P.; Bernardino, A. M. R.; Santos, D. O.; Castro, H. C. *Bioorg. Med. Chem.* **2008**, *16*, 8196–8204. DOI: <https://doi.org/10.1016/j.bmc.2008.07.035>.
- 7.(a) Fugel, W.; Oberholzer, A. E.; Gschloessl, B.; Dzikowski, R.; Pressburger, N.; Preu, L.; Pearl, L. H.; Baratte, B.; Ratin, M.; Okun, I.; Doerig, C.; Kruggel, S.; Lemcke, T.; Meijer, L.; Kunick, C. *J. Med. Chem.* **2013**, *56*, 264–275. DOI: <https://doi.org/10.1021/jm301575n>. (b) Verma, A. K.; Kotla, S. K. R.; Choudhary, D.; Patel, M.; Tiwari, R. K. *J. Org. Chem.* **2013**, *78*, 4386–4401. DOI: <https://doi.org/10.1021/jo400400c>.
8. Dayanandan, N.; Paulsen, J. L.; Viswanathan, K.; Keshipeddy, S.; Lombardo, M. N.; Zhou, W.; Lamb, K. M.; Sochia, A. E.; Alverson, J. B.; Priestley, N. D.; Wright, D. L.; Anderson, A. C. *J. Med. Chem.* **2014**, *57*, 2643–2656. DOI: <https://doi.org/10.1021/jm401916j>.
9. Jain, K. S.; Khedkar, V. M.; Arya, N.; Rane, P. V.; Chaskar, P. K.; Coutinho, E. C. *Eur. J. Med. Chem.* **2014**, *77*, 166–175. DOI: <https://doi.org/10.1016/j.ejmech.2014.02.066>.
10. Serpi, M.; Ferrari, V.; Pertusati, F. *J. Med. Chem.* **2016**, *59*, 10343–10382. DOI: <https://doi.org/10.1021/acs.jmedchem.6b00325>.
11. McCarty, T. P.; White, C. M.; Pappas, P. G. *Infect. Dis. Clin. North Am.* **2021**, *35*, 389–413. DOI: <https://doi.org/10.1016/j.idc.2021.03.007>.
12. Pristov, K. E.; Ghannoum, M. A. *Clin. Microbiol. Infect.* **2019**, *25*, 792–798. DOI: <https://doi.org/10.1016/j.cmi.2019.03.028>.
13. Earle, K.; Valero, C.; Conn, D. P.; Vere, G.; Cook, P. C.; Bromley, M. J.; Bowyer, P.; Gago, S. *Virulence* **2023**, *14*, 2172264. DOI: <https://doi.org/10.1080/21505594.2023.2172264>.
14. Khan, A. A.; Farooq, F.; Jain, S. K.; Golinska, P.; Rai, M. *Microb. Ecol.* **2022**, *84*, 1236–1244. DOI: <https://doi.org/10.1007/s00248-021-01913-6>.
15. Prakash, S.; Kumar, A. *J. Basic Microbiol.* **2023**, *63*, 119–127. DOI: <https://doi.org/10.1002/jobm.202200334>.
16. Dam, P.; Cardoso, M. H.; Mandal, S.; Franco, O. L.; Sağıroğlu, P.; Polat, O. A.; Kokoglu, K.; Mondal, R.; Mandal, A. K.; Ocsoy, I. *Travel Med. Infect. Dis.* **2023**, *52*, 102557. DOI: <https://doi.org/10.1016/j.tmaid.2023.102557>.
17. Góralaska, K.; Blaszkowska, J.; Dzikowicz, M. *Infection* **2018**, *46*, 443–459. DOI: <https://doi.org/10.1007/s15010-018-1152-2>.
18. Ando, M.; Arima, K.; Yoneda, R.; Tamura, M. *Am. Rev. Respir. Dis.* **1991**, *144*, 765–769. DOI: <https://doi.org/10.1164/ajrccm/144.4.765>.
19. Hemalatha, K.; Selvin, J.; Girija, K. *Asian J. Pharm. Res.* **2018**, *8*, 125–132. DOI: <https://doi.org/10.5958/2231-5691.2018.00022.9>.
20. Hassan, M.; Ashraf, Z.; Abbas, Q.; Raza, H.; Seo, S.-Y. *Interdiscip. Sci. Comput. Life Sci.* **2018**, *10*, 68–80. DOI: <https://doi.org/10.1007/s12539-016-0171-x>.

21. Ramírez-Villalva, A.; González-Calderón, D.; Rojas-García, R. I.; González-Romero, C.; Tamariz-Mascarúa, J.; Morales-Rodríguez, M.; Zavala-Segovia, N.; Fuentes-Benites, A. *Med. Chem. Comm.* **2017**, 8, 2258–2262. DOI: <https://doi.org/10.1039/C7MD00442G>.
22. Chandrasekaran, S. *Click Reactions in Organic Synthesis*, Ed., Wiley-VCH, **2016**.
23. Vanjare, B. D.; Seok Eom, Y.; Raza, H.; Hassan, M.; Hwan Lee, K.; Ja Kim, S. *Bioorg. Med. Chem.* **2022**, 63, 116745. DOI: <https://doi.org/10.1016/j.bmc.2022.116745>.
24. Rex, J. H. *Reference Method for Broth Dilution Antifungal Susceptibility Testing of Yeasts: Approved Standard*, 3. ed., Ed., Clinical and Laboratory Standards Institute, **2008**.
25. Rex, J. H. *Reference Method for Broth Dilution Antifungal Susceptibility Testing of Filamentous Fungi: Approved Standard*, 2. ed., Ed., Clinical and Laboratory Standards Institute, **2008**.